UC Santa Barbara
UC Santa Barbara Previously Published Works

Title
Infrasonic crackle and supersonic jet noise from the eruption of Nabro Volcano, Eritrea

Permalink
https://escholarship.org/uc/item/23c8b0c9

Journal
Geophysical Research Letters, 40(16)

ISSN
0094-8276

Authors
Fee, D
Matoza, RS
Gee, KL
et al.

Publication Date
2013-08-28

DOI
10.1002/grl.50827

Peer reviewed

Infrasonic crackle and supersonic jet noise from the eruption of Nabro Volcano, Eritrea

David Fee,[1] Robin S. Matoza,[2] Kent L. Gee,[3] Tracianne B. Neilsen,[3] and Darcy E. Ogden[2]

[1] The lowermost portion of an explosive volcanic eruption column is considered a momentum-driven jet. Understanding volcanic jets is critical for determining eruption column dynamics and mitigating volcanic hazards; however, volcanic jets are inherently difficult to observe due to their violence and opacity. Infrasound from the 2011 eruption of Nabro Volcano, Eritrea has waveform features highly similar to the "crackle" phenomenon uniquely produced by man-made supersonic jet engines and rockets and is characterized by repeated asymmetric compressions followed by weaker, gradual rarefactions. This infrasonic crackle indicates that infrasound source mechanisms in sustained volcanic eruptions are strikingly similar to jet noise sources from heated, supersonic jet engines and rockets, suggesting that volcanologists can utilize the modeling and physical understandings of man-made jets to understand volcanic jets. The unique, distinctive infrasonic crackle from Nabro highlights the use of infrasound to remotely detect and characterize hazardous eruptions and its potential to determine volcanic jet parameters. **Citation:** Fee, D., R. S. Matoza, K. L. Gee, T. B. Neilsen, and D. E. Ogden (2013), Infrasonic crackle and supersonic jet noise from the eruption of Nabro Volcano, Eritrea, *Geophys. Res. Lett.*, *40*, doi:10.1002/grl.50827.

1. Introduction

[2] Detection and characterization of volcanic eruption flow parameters is critical for hazard mitigation, but the difficulty in obtaining accurate, real-time, and/or continuous measurements of volcanic eruption columns is well known [*Mastin et al.*, 2009]. Volcanoes are sources of high-amplitude, varied acoustic signals, particularly at frequencies below 20 Hz (termed infrasound) [*Fee and Matoza*, 2013]. Linking geophysical signals, such as infrasound, to volcanic eruption features can provide key insight into eruption column dynamics and therefore hazard mitigation [*Prejean and Brodsky*, 2011; *Fee and Matoza*, 2013]. For example, recent work has suggested that infrasound from large, sustained volcanic eruptions resembles a low-frequency form of the sound from man-made jet engine flows (jet noise) [*Matoza et al.*, 2009]. Understanding the relationship between infrasound and volcanic jet flow features may permit real-time, continuous characterization of volcanic eruption columns.

[3] Jet noise is the sound produced by interactions between the turbulent exhaust flow from, e.g., aircraft and rockets and the ambient air. As part of extensive efforts to characterize and reduce jet noise [*Tam*, 1998], a phenomenon known as "crackle" has been identified as an "annoying" [*Ffowcs Williams et al.*, 1975] and "dominant" [*Krothapalli et al.*, 2000] component of the overall radiation from supersonic jet flows. Crackle is defined as intense sound characterized by the repeated occurrence of asymmetric pressure pulses of sharp, high-amplitude compressions followed by weaker, gradual rarefactions [*Ffowcs Williams et al.*, 1975; *Krothapalli et al.*, 2000]. The term crackle connotes a "snapping" or "popping" sound in the audible region and has been described [*Ffowcs Williams et al.*, 1975] as similar to the sound of repeated and irregular ripping of paper. Beginning with *Ffowcs Williams et al.* [1975], numerous studies have correlated crackle with considerable positive waveform skewness. The skewness (S) of the waveform amplitude distribution (asymmetry) is defined as the normalized third central moment of the probability density function (PDF) of the time waveform amplitude (Figures 1c–1d). Whereas a Gaussian PDF ($S = 0$) has been associated with low-amplitude noise radiating from subsonic jets, positively skewed distributions have been observed from supersonic jets produced by laboratory-scale nozzles [*Krothapalli et al.*, 2000; *Petitjean et al.*, 2006], full-scale military aircraft engines [*McInerny et al.*, 2006; *Gee et al.*, 2007] and solid rocket motors and launch vehicles [*McInerny*, 1996; *Gee et al.*, 2009], as well as in numerical simulations of supersonic jets [*Nichols et al.*, 2012]. Waveform skewness is greater in the vicinity of the peak noise direction and increases with Mach number, temperature, and amplitude [*Krothapalli et al.*, 2000; *Petitjean et al.*, 2006], and has been observed sufficiently close to the jet to be considered a source phenomenon [*Gee et al.*, 2013]. Although still under investigation, crackle may originate from repeated microexplosions occurring from cold ambient air entrained in the hot jet [*Krothapalli et al.*, 2000; *Nichols et al.*, 2012]. Recent studies have examined acoustic shocks in crackle using waveform derivative statistics [*McInerny et al.*, 2006; *Petitjean et al.*, 2006; *Gee et al.*, 2013], which requires relatively high data sampling rates not typically available for volcano infrasound. Herein, our analyses
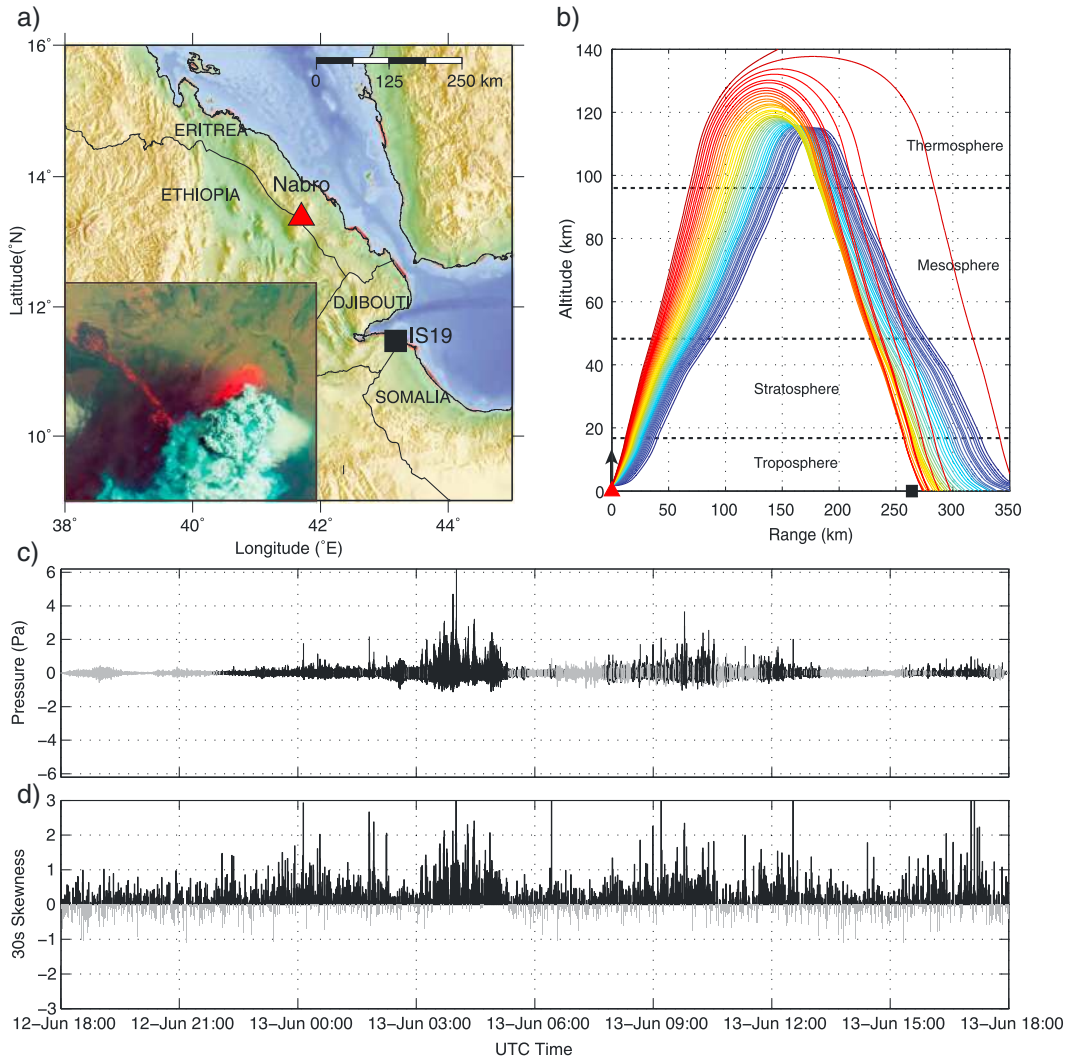
Figure 1. Map of Nabro and IS19, followed by infrasound data and skewness. (a) Map of East Africa, including Nabro Volcano, Eritrea (red triangle), and the IS19 infrasound array (black square). Inset image is an EO-1 ALI satellite image of the Nabro eruption on 27 June 2011, credit: NASA's Earth Observatory. (b) Ray tracing from Nabro to IS19. Sound energy is predicted to propagate to the thermosphere and refract down to near IS19. The black arrow above Nabro indicates the downstream volcanic jetting direction. Rays are colored by their launch angle. (c) IS19 L1 infrasound data beginning 12 June 2011 1800 UTC filtered between 0.1 and 8 Hz. Waveform segments from Nabro are colored black, while noise is colored gray. (d) Skewness calculated at 30 s intervals, with positive skewness black and negative skewness gray. The eruption times correspond to increased infrasound amplitude and positive skewness.

focus on how the infrasonic pressure waveform statistics from Nabro Volcano are consistent with man-made crackling jets.

2. The 2011 Eruption of Nabro Volcano, Eritrea

[4] Nabro Volcano, Eritrea (Figure 1a) erupted unexpectedly and explosively on 12 June 2011. Although highly elevated seismicity was detected by regional seismic networks in East Africa in the days preceding the eruption (14 earthquakes $M > 4.5$), the lack of any local or regional volcano monitoring in this remote region [*Smithsonian*, 2011] and no known historical eruptive activity [*Wiart and Oppenheimer*, 2005] created confusion for civil aviation authorities in the early hours of the eruption. In fact, the eruption was initially attributed to Dubbi Volcano ~25 km away [*Bojanowski*, 2011; *Smithsonian*, 2011]. As detected by satellite and

ground-based lidar, the relatively ash-poor, gas-rich eruption produced one of the largest eruptive SO_2 masses (~4.5 Tg) since Mt. Pinatubo in 1991 and the single largest SO_2 column ever retrieved from space [*Clarisse et al.*, 2011; *Theys et al.*, 2013]. The highest emissions reached the lowermost stratosphere (~19 km altitude), circled the globe, and caused small but detectable climate changes [*Bourassa et al.*, 2012]. The eruption killed seven people, displaced thousands, damaged crops, and disrupted air traffic. Extensive volcanic emissions and lava flows persisted through mid-June then continued at a lower level until mid-July [*Smithsonian*, 2011].

3. Infrasound Data and Methods

[5] The Nabro eruption produced abundant low-frequency sound that was recorded by two infrasound arrays in the region: IS19 (Djibouti) and IS32 (Kenya). These arrays are

2
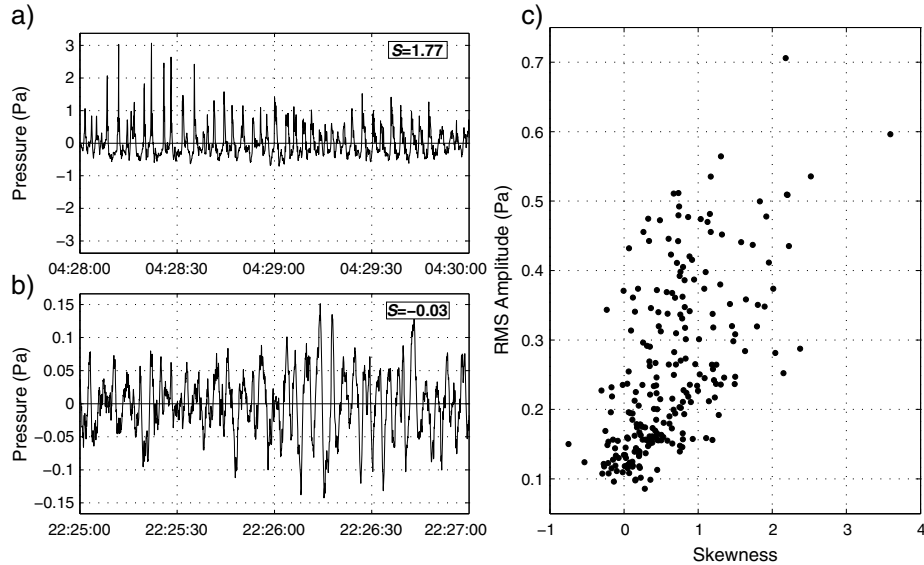
Figure 2. Two minute infrasound examples from Nabro. (a) High-amplitude skewed infrasound (June 13) showing repeated sharp compressions and more gradual rarefactions characteristic of crackle. (b) Lower-amplitude, nonskewed infrasound from Nabro (June 14). (c) 30 s RMS amplitude versus skewness values between 03:00 and 05:00 UTC on 13 June. A general positive correlation exists between increased amplitude and skewness, similar to that from supersonic aircraft and rockets.

part of the International Monitoring System (IMS) of the Comprehensive Nuclear-Test-Ban Treaty Organization. The IS19 array (Figure 1a) is located 264 km southeast of Nabro and recorded the eruption with high signal-to-noise. It provides the most detailed eruption chronology available including eruption onset, duration, and changes in intensity. IS32 is much farther away at 1708 km and detailed waveform features would likely be lost at this distance due to numerous ground reflections and multipathing [*Fee and Matoza*, 2013].

[6] Infrasound data at IS19 were recorded on an eight element, 2 km aperture array of MB-2005 microbarometers. Infrasound array detections are determined by first filtering the data between 0.1–8 Hz using a 4 pole, acausal Butterworth filter. The data are then divided into 30 s windows with 50% overlap, followed by computation of the trace velocity and azimuth using a least squares method [*Szuberla and Olson*, 2004]. Each data window is then colored by the Fisher Statistic (Figure 1c) [*Melton and Bailey*, 1957]. All other infrasound data shown are from the IS19 L1 element and are filtered similarly. Ray tracing is performed using classical geometric acoustics techniques and a plane wave assumption [*Blom and Waxler*, 2012], with rays launched between 1° and 45° from the horizontal axis at 1° intervals from a source height of 2 km (the volcanic vent elevation). The NRL-G2S [*Drob et al.*, 2003] atmospheric specifications are used in the propagation modeling.

4. Results and Analyses

[7] We perform ray tracing to model infrasound propagation from Nabro to IS19 (Figure 1b). Sound energy propagates up to the thermosphere before it is refracted back down between ~110 and 130 km altitude. Rays are predicted to reach the ground just beyond Nabro at 274 km distance with a travel time of 1237 s (~20.6 min). Although the predicted rays do not directly reach the station, the modeling does not account for frequency-dependent propagation effects such as diffraction and the separation distance is within

the accuracy limitations of the atmospheric specifications [*Drob et al.*, 2003; *Matoza et al.*, 2011; *Assink et al.*, 2012]. Thermospheric propagation is consistent with the observed high trace velocities (mean 0.38 km/s, Figure S1b in the supporting information) and is expected at this range and equatorial location [*Assink et al.*, 2012].

[8] Infrasound from the first few days of the eruption consists of high-amplitude signals lasting a few hours. Figure 1c displays 24 h of IS19 infrasound data beginning 12 June 18:00 UTC, with pressure waveform segments determined to be from Nabro shown in black and other noise shown in gray (see Figure S1 for array processing details). Infrasound from Nabro begins on 12 June ~21:44 UTC, continues until 13 June ~05:00 UTC, and then diminishes before resuming again around 10:00 UTC. Note that high-amplitude infrasound from Nabro continued for the next few days and was coincident with voluminous, high-altitude volcanic emissions, as described by other studies [*Fee et al.*, 2010; *Dabrowa et al.*, 2011; *Matoza et al.*, 2011; *Fee and Matoza*, 2013; *Fromm et al.*, 2013]. The Nabro infrasound in Figure 1c has a striking positive asymmetry (greater positive pressure values than negative), which suggests the potential for skewness analysis to quantify this characteristic. The IS32 data does not contain noticeable asymmetry, likely due to its much greater distance.

[9] Skewness from the pressure data in Figure 1c was calculated over 30 s intervals and is displayed in Figure 1d, with black indicating periods during which $S > 0$. Comparison of Figures 1c–d shows that skewness values are typically positive and high ($S > 0.5$) for periods corresponding to high-amplitude infrasound from Nabro, peaking at $S = 3.5$ at ~04:00 UTC. For reference, $S > 0.4$ was suggested as a threshold for defining crackle for high-power jet engines [*Ffowcs Williams et al.*, 1975]. We found that calculated skewness values are relatively insensitive to changes in interval length.

[10] Skewness and pressure amplitude from Nabro are positively correlated. First, Figure 2 shows examples of low- and high-amplitude waveform segments originating

3
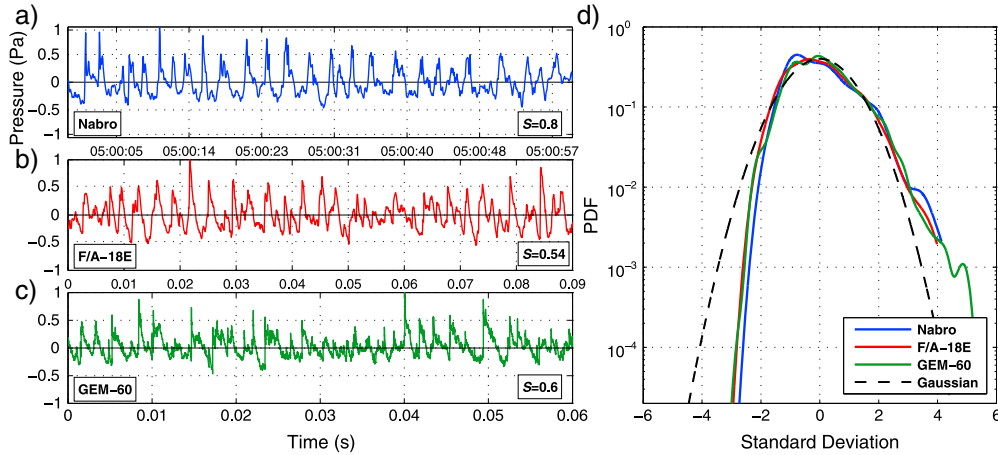
Figure 3. Comparison of Nabro infrasound with heated, supersonic aircraft and rocket data. Waveforms for (a) Nabro, (b) F/A-18E Super Hornet jet engine, and (c) GEM-60 solid rocket. All three waveforms have similar features including high, positive skewness values. Data in Figures 3b and 3c have been normalized. (d) PDF of the pressure waveforms in Figures 3c–3d normalized by their standard deviation. All three waveforms have similar skewed distributions with long positive tails. A Gaussian PDF is shown in black for comparison. Note the PDFs are plotted on a log scale to emphasize the tails of the distributions [*Gee et al.*, 2007].

from Nabro. Figure 2a highlights 2 min of high-amplitude, high-skewness infrasound characterized by repeated, impulsive compressions followed by weaker, longer duration rarefactions. Figure 2b shows a low-amplitude, near-zero skewness segment from 14 June. Figure 2c shows explicitly the correlation between pressure amplitude and skewness; large skewness values only occur during high-amplitude periods. This correlation of skewness with pressure amplitude is similar to that observed from supersonic jet engines [*McInerny et al.*, 2006] and rockets [*McInerny*, 1996], indicating that the crackle in the high-amplitude infrasound is a source feature and not an infrasound propagation effect.

5. Comparison of Nabro Infrasound With Jet and Rocket Engine Data

[11] We further illustrate the similarity between the Nabro infrasound with crackle by directly comparing the infrasound with audible noise from heated supersonic aircraft and rocket engines. Data from tests of an F/A-18E Super Hornet jet engine [*Gee et al.*, 2005] and GEM-60 rocket motor [*Gee et al.*, 2009] are selected. The F/A-18E data are from a test where the tied-down aircraft was run at afterburner and recordings were made using a 6.35 mm Bruel and Kjaer 4938 condenser microphone [*Gee et al.*, 2007]. The GEM-60 is a solid-fuel rocket used as a booster for the Delta IV launch vehicle and has an average vacuum thrust of 828,000 N. The rocket is 16.2 m in length with a 1.52 m diameter nozzle. The GEM-60 solid rocket data were recorded using a GRAS 6.35 mm 40BD pressure microphone [*Gee et al.*, 2009]. Figures 3a–c displays 1 min of Nabro infrasound along with time-scaled audible waveforms from the F/A-18E jet and GEM-60 rocket. Supersonic aircraft and rocket data are normalized and then scaled to match the repeat frequency of the Nabro crackle pulses. All three waveforms have high positive skewness values and are characterized by impulsive asymmetric compressions and lower amplitude, longer rarefactions. The GEM-60 and Nabro data show particular similarity. The similarity is strengthened by Figure 3d, which compares

the PDFs of the waveforms in Figures 3a–c with that of a Gaussian distribution. PDFs were computed using a normal kernel function estimate method. A strong similarity exists between the Nabro, military aircraft, and rocket PDF distributions, with all three being positively skewed with long positive tails. Additional waveform segments have comparable skewness values and PDF distributions. The agreement between Nabro infrasound and man-made supersonic jet noise is remarkable given the differences in the size, thrust, temperature, etc., and point to the promise of applying the body of knowledge about supersonic jet and rocket noise to better characterize volcanic infrasound.

6. Conclusions

[12] We have shown that acoustic waveforms from an explosive volcanic eruption are highly similar to those from supersonic jet flows. These unique waveforms indicate that volcanic jets can make sound in similar ways to man-made supersonic jet and rocket engines. Although crackle is commonly observed from heated, supersonic jet and rocket engines, this is the first documented case of crackle from a volcano. We speculate that the uniqueness of the Nabro infrasound may be due to the gas-rich/ash-poor nature and explosiveness of the eruption. These types of eruptions are rare and thus challenging to record with infrasound sensors, particularly at close range. However, the expansion of the IMS network and deployment of additional infrasound stations in recent years provide greater opportunities to record large eruptions [*Fee et al.*, 2010; *Matoza et al.*, 2011]. Crackle is also directed downstream of the jet and thus will propagate out at high angles into the atmosphere, restricting the regions where it may be detected. *McGimsey and Dorava* [1994] observed continuous shock waves being emitted from the base of the 1992 Mt. Spurr eruption, which is consistent with the flow process required to produce crackle. Note they heard no sound from the volcano from their sideline angle to the eruption column even though they were only a few kilometers away. Because the identification of crackle via the

4

skewness is fairly straightforward, high waveform skewness could be used, in conjunction with other characteristics such as the jet noise similarity spectra [*Matoza et al.*, 2009], to rapidly identify hazardous volcanic jetting in an acoustic early warning system [*Fee et al.*, 2010; *Matoza et al.*, 2011].

[13] The unique, distinctive infrasonic crackle from Nabro suggests that the volcanic jet was supersonic relative to the ambient sound speed (~330 m/s), not unexpected for explosive eruptions of this size [*Sparks et al.*, 1997]. Determination of the volcanic jet velocity has important implications for understanding the eruption column dynamics including mass flux, plume height, and ash dispersal. Future field, laboratory, and numerical work to better understand the relationship between infrasound and volcanic jets could lead to detailed information on the eruption column which would have significant benefits for hazard mitigation and volcano modeling. Correlating changes in crackle properties with changes in volcanic jet features shows particular promise, such as the observed increase in skewness with increasing Mach number and temperature for laboratory jets [*Krothapalli et al.*, 2000; *Petitjean et al.*, 2006].

References

Assink, J. D., R. Waxler, and D. Drob (2012), On the sensitivity of infrasonic traveltimes in the equatorial region to the atmospheric tides, *J. Geophys. Res.*, *117*, D01110, doi:10.1029/2011JD016107.

Blom, P., and R. Waxler (2012), Impulse propagation in the nocturnal boundary layer: Analysis of the geometric component, *J. Acoust. Soc. Am.*, *131*(5), 3680–3690, doi:10.1121/1.3699174.

Bojanowski, A. (2011), Volcano mix-up, *Nat. Geosci.*, *4*(8), 495, doi:10.1038/ngeo1222.

Bourassa, A. E., A. Robock, W. J. Randel, T. Deshler, L. A. Rieger, N. D. Lloyd, E. J. Llewellyn, and D. A. Degenstein (2012), Large volcanic aerosol load in the stratosphere linked to Asian monsoon transport, *Science*, *337*(6090), 78–81, doi:10.1126/science.1219371.

Clarisse, L., D. Hurtmans, C. Clerbaux, J. Hadji-Lazaro, Y. Ngadi, and P. F. Coheur (2011), Retrieval of sulphur dioxide from the infrared atmospheric sounding interferometer (IASI), *Atmos. Meas. Tech. Discuss.*, *4*(6), 7241–7275, doi:10.5194/amtd-4-7241-2011.

Dabrowa, A. L., D. N. Green, A. C. Rust, and J. C. Phillips (2011), A global study of volcanic infrasound characteristics and the potential for long-range monitoring, *Earth Planet. Sci. Lett.*, *310*(3–4), 369–379, doi:10.1016/j.epsl.2011.08.027.

Drob, D. P., J. M. Picone, and M. Garces (2003), Global morphology of infrasound propagation, *J. Geophys. Res.*, *108*(D21), 4680, doi:10.1029/2002jd003307.

Fee, D., and R. S. Matoza (2013), An overview of volcano infrasound: From Hawaiian to Plinian, local to global, *J. Volcanol. Geotherm. Res.*, *249*, 123–139, doi:10.1016/j.jvolgeores.2012.09.002.

Fee, D., A. Steffke, and M. Garces (2010), Characterization of the 2008 Kasatochi and Okmok eruptions using remote infrasound arrays, *J. Geophys. Res.*, *115*, D00L10, doi:10.1029/2009JD013621.

Ffowcs Williams, J. E., J. Simson, and V. J. Virchis (1975), "Crackle": An annoying component of jet noise, *J. Fluid Mech.*, *71*(2), 251–271.

Fromm, M., G. Nedoluha, and Z. Charvát (2013), Comment on "large volcanic aerosol load in the stratosphere linked to Asian monsoon transport", *Science*, *339*(6120), 647, doi:10.1126/science.1228605.

Gee, K. L., T. B. Gabrielson, A. A. Atchley, and V. W. Sparrow (2005), Preliminary analysis of nonlinearity in military jet aircraft noise propagation, *AIAA Journal*, *43*(6), 1398–1401, doi:10.2514/1.10155.

Gee, K. L., V. W. Sparrow, A. Atchley, and T. B. Gabrielson (2007), On the perception of crackle in high-amplitude jet noise, *AIAA Journal*, *45*(3), 593–598, doi:10.2514/1.26484.

Gee, K. L., J. H. Giraud, J. D. Blotter, and S. D. Sommerfeldt (2009), Energy-based acoustical measurements of rocket noise, *15th AIAA/CEAS Aeroacoustics Conference* (*30th AIAA Aeroacoustics Conference*), doi:10.2514/6.2009-316510.2514/6.2009-3165.

Gee, K. L., T. B. Neilsen, J. M. Downing, M. M. James, R. L. McKinley, R. C. McKinley, and A. T. Wall (2013), Near-field shock formation in noise propagation from a high-power jet aircraft, *J. Acoust. Soc. Am.*, *133*(2), EL88–93, doi:10.1121/1.4773225.

Krothapalli, A., L. Venkatakrishnan, and L. Lourenco (2000), Crackle: A dominant component of supersonic jet mixing noise, *AIAA Paper*, *2000-2024*.

Mastin, L. G., et al. (2009), A multidisciplinary effort to assign realistic source parameters to models of volcanic ash-cloud transport and dispersion during eruptions, *J. Volcanol. Geotherm. Res.*, *186*(1–2), 10–21, doi:10.1016/j.jvolgeores.2009.01.008.

Matoza, R. S., D. Fee, M. A. Garces, J. M. Seiner, P. A. Ramon, and M. A. H. Hedlin (2009), Infrasonic jet noise from volcanic eruptions, *Geophys. Res. Lett.*, *36*, L08303, doi:10.1029/2008GL036486.

Matoza, R. S., A. Le Pichon, J. Vergoz, P. Herry, J. Lalande, H. Lee, I. Che, and A. Rybin (2011), Infrasonic observations of the June 2009 Sarychev Peak eruption, Kuril Islands: Implications for infrasonic monitoring of remote explosive volcanism, *J. Volcanol. Geotherm. Res.*, *200*, 35–48, doi:10.1016/j.jvolgeores.2010.11.022.

McGimsey, R., and J. Dorava (1994), Video of the August 18, 1992, eruption of Crater Peak vent on Spurr volcano, *Alaska*: *US Geological Survey Open-File Report*, 94–105.

McInerny, S., M. Downing, C. Hobbs, M. James, and M. Hannon (2006), Metrics that characterize nonlinearity in jet noise, *Innovations in Nonlinear Acoustics Proceedings of 17th ISNA* 838, pp. 560–563, doi:10.1063/1.2210418.

McInerny, S. A. (1996), Launch vehicle acoustics Part 2: Statistics of the time domain data, *J. Aircraft*, *33*, 518–523.

Melton, B. S., and L. F. Bailey (1957), Multiple signal correlators, *Geophysics*, *22*, 565, doi:10.1190/1.1438390.

Nichols, J. W., S. K. Lele, F. E. Ham, S. Martens, and J. T. Spyropoulos (2012), Crackle noise in heated supersonic jets, *Proceedings of ASME Turbo Expo 2012*, Paper No. GT2012-69624.

Petitjean, B., K. Viswanathan, and D. McLaughlin (2006), Acoustic pressure waveforms measured in high speed jet noise experiencing nonlinear propagation, *International Journal of Aeroacoustics*, *5*(2), 193–215, doi:10.1260/147547206777629835.

Prejean, S. G., and E. E. Brodsky (2011), Volcanic plume height measured by seismic waves based on a mechanical model, *J. Geophys. Res.*, *116*, B01306, doi:10.1029/2010JB007620.

Smithsonian, I. (2011), Nabro, *Bulletin of the Global Volcanism Network* (*BVGN*), *36*(9).

Sparks, R. S. J., M. I. Bursik, S. N. Carey, J. S. Gilbert, L. S. Glaze, H. Siggurdsson, and A. W. Woods (1997), *Volcanic Plumes*, 574 pp., John Wiley and Sons, New York.

Szuberla, C. A. L., and J. V. Olson (2004), Uncertainties associated with parameter estimation in atmospheric infrasound arrays, *J. Acoust. Soc. Am.*, *115*(1), 253–258, doi:10.1121/1.1635407.

Tam, C. K. W. (1998), Jet noise: Since 1952, *Theor. Comput. Fluid Dyn.*, *10*(1–4), 393–405.

Theys, N., et al. (2013), Volcanic SO2 fluxes derived from satellite data: A survey using OMI, GOME-2, IASI and MODIS, *Atmos. Chem. Phys.*, *13*(12), 5945–5968, doi:10.5194/acp-13-5945-2013.

Wiart, P., and C. Oppenheimer (2005), Large magnitude silicic volcanism in north Afar: The Nabro Volcanic Range and Ma'alalta volcano, *Bull. Volcanol.*, *67*(2), 99–115, doi:10.1007/s00445-004-0362-x.